American Mineralogist, Volume 91, pages 115–119, 2006

First-principles study of the OH-stretching modes of gibbsite

Etienne Balan,[1,2,*] Michele Lazzeri,[2] Guillaume Morin,[2] and Francesco Mauri[2]

[1]UR GEOTROPE, Institut de Recherche pour le Développement (IRD), 213 rue La Fayette, 75480, Paris cedex 10, France
[2]Institut de Minéralogie et Physique des Milieux Condensés (IMPMC), UMR CNRS 7590, Universités Paris VI et VII, IPGP, 4 Place Jussieu, 75252 Paris Cedex 05, France

Abstract

The theoretical infrared (IR) and Raman spectra of gibbsite [α-$Al(OH)_3$] were computed using ab initio quantum mechanical calculations. The low-frequency dielectric tensor and the Raman tensors of gibbsite were determined using linear response theory. The transmission powder IR spectrum was found to strongly depend on the shape of the gibbsite particles. In the region of the OH-stretching bands, an excellent agreement between theory and experiment was obtained, providing an unambiguous interpretation of the OH bands in terms of vibrational modes. In contrast, the assignment of the bands observed at lower frequency is complicated by the significant overlap between neighboring bands together with their sensitivity to particle shape.

Keywords: IR spectroscopy, Raman spectroscopy, quantum mechanical calculation, gibbsite

Introduction

Gibbsite, α-$Al(OH)_3$, is the most common aluminum ore mineral. It mainly occurs in bauxites and lateritic soils, as a result of the intense weathering of aluminous minerals in tropical climates (Tardy 1993). Its surface properties have attracted much attention as a model system to investigate the reactivity of mineral surfaces in soils and sediments (e.g., Kubicki and Apitz 1998; Jodin et al. 2004). The high-pressure behavior of gibbsite has recently been investigated to gain some insight to the phase transitions affecting hydrous phases in subduction zones (Johnston et al. 2002; Liu et al. 2004). Some theoretical studies, motivated by the industrial use of gibbsite, have also addressed its thermal stability (Digne et al. 2002) and the effect of alkaline cation incorporation on its crystal morphology (Fleming et al. 2001).

Identification of gibbsite in complex mineral mixtures or synthetic samples can be readily performed by using infrared or Raman spectroscopy (e.g., Farmer 1974; Ruan et al. 2001). In particular, the OH-stretching modes produce a series of well-defined bands observed between 3200 and 3700 cm^{-1}. This pattern is related to the stretching vibration of the six non-equivalent OH groups of the gibbsite structure. According to factor group analysis, each OH group is expected to produce four vibrational modes referred to as A_g, B_g, A_u, or B_u, corresponding to the four irreducible representations of the C_{2h} point group. Because of the inversion symmetry, the two centro-symmetric A_g and B_g modes are Raman-active modes, whereas the anti-symmetric A_u and B_u modes are infrared active (Wang and Johnston 2000). Neglecting the coupling between the vibration of non-equivalent OH groups and the coupling between the vibration of OH groups belonging to different layers, Raman and infrared active bands are expected to be degenerate and a one-to-one assignment of the experimental bands to the six non-equivalent OH groups has been proposed (Wang and Johnston 2000). However, the calculation of vibrational modes by Gale et al. (2001) has suggested that some of these modes result from mixing between the vibration of non-equivalent OH groups. Unfortunately, the limited agreement observed between theoretical and experimental frequencies makes it difficult to unambiguously interpret the vibrational spectra of gibbsite in the range of OH-stretching modes. In addition, recent theoretical modeling of the vibrational spectra of layered minerals, such as the kaolinite-group minerals, has shown that the interlayer coupling for modes polarized perpendicular to the layers is far from insignificant (Balan et al. 2005). Finally, the experimental study of Phambu et al. (2000) has shown that the infrared spectrum of gibbsite samples strongly depends on the shape of the gibbsite particles, suggesting that OH groups located at the surface of the gibbsite particles contribute significantly to the spectrum.

In a polar crystal, certain vibrational modes can be coupled with a macroscopic electric field. If this is the case, optical vibrations can depend on the macroscopic polarizability of the system, and thus, on the macroscopic shape of the system. Whereas the vibrational properties of the gibbsite surface were successfully simulated using isolated small clusters (e.g., Kubicki and Apitz 1998; Kubicki 2001), this approach does not allow for a proper description of the macroscopic polarizability of the bulk. In the present study, we theoretically investigated the infrared and Raman spectra of gibbsite using ab initio quantum mechanical calculations, considering both the frequency and the intensity of vibrational bands. We used periodic boundary conditions, allowing for a complete description of the crystal polarizability. The low-frequency dielectric tensor and Raman tensors were determined using the density functional perturbation theory (Baroni et al. 2001; Lazzeri and Mauri 2003). The influence of the particle shape on the IR spectrum turns out to be an essential ingredient to provide an unambiguous interpretation of the OH bands in terms of vibrational modes.

* E-mail: balan@lmcp.jussieu.fr

0003-004X/06/0001–115$05.00/DOI: 10.2138/am.2006.1922

METHODS

Experimental details

Room-temperature IR spectra were recorded from a synthetic gibbsite sample (Amag 25) precipitated from the sodium hydroxide solution of the Bayer process. The gibbsite particles have a micrometric size, with a euhedral shape ranging from platy to nearly equant (Fig. 1). Approximately 2 mg of dried sample was gently ground with 300 mg of dry KBr and pressed to produce a rigid disk. The transmission IR spectrum of the disk was recorded between 250 and 4000 cm^{-1} at room temperature using a Nicolet Magna 560 FTIR spectrometer with a resolution of 2 cm^{-1}.

Computational details

Calculations were performed within the Density Functional Theory (DFT) framework, using the generalized gradient approximation to the exchange-correlation functional as proposed by Perdew et al. (1996). The ionic cores were described by norm-conserving pseudo-potentials (Troullier and Martins 1991) in the Kleinman-Bylander form (Kleinman and Bylander 1982). The electronic wave-functions were expanded in plane-waves up to a 80 Ry cutoff. Because of the large size of the unit cell, which contains 56 atoms, the electronic integration was performed by restricting the sampling of the Brillouin zone to its center (Γ point) only. Atomic relaxations were performed with the PWSCF code (Baroni et al.; http://www.pwscf.org) until the residual forces on atoms were less than 10^{-3} Ry/Å.

In a polar insulator, such as gibbsite, infrared and Raman spectra can be obtained knowing the analytical part of the dynamical matrix and dielectric quantities such as the Born effective charges and the electronic dielectric tensor. These quantities were calculated using the linear response theory (Baroni et al. 2001). They were derived from the second-order derivatives of the total energy with respect to atomic displacements and/or an external uniform electric field, using the PHONON code (Baroni et al. 2001; http://www.pwscf.org). Previous calculations concerning 1:1 phyllosilicates have demonstrated the accuracy of this approach for modeling the vibrational properties of hydrous minerals (Balan et al. 2001, 2002, 2005).

In general, the vibrational frequencies (which determine the peak positions in both infrared and Raman spectra) can be influenced by the coupling of the atomic vibrations with a macroscopic electric field (LO-TO splitting). In such a situation, the vibrational frequencies depend on the macroscopic shape of the measured particles. In the IR measurements, gibbsite particles have a size smaller than the incident-light wavelength (ca. 3 μm) and appear with very different shapes (Fig. 1). Thus, the frequency of the vibrational modes affected by the particle shape will not appear as well-defined peaks but as broadened peaks resulting from the contribution of particles with different shapes. To describe the frequency dependence from the particle shape, we have determined the powder infrared gibbsite spectrum using a model similar to the one developed by Balan et al. (2001). This model, developed for thin disks, can be easily extended to small particles of arbitrary ellipsoidal shape because in both cases the electric and polarization fields are homogeneous inside the particle. In the present work, we considered the two limiting cases of particles with a thin-disk shape and particles with a spherical shape. Finally, the Raman spectrum of a single crystal of gibbsite was computed in the OH-stretching range for the various polarizations reported by Wang and Johnston (2000) and using the approach detailed in Balan et al. (2005). The Raman tensors was computed using the second-order response to DFT as in Lazzeri and Mauri (2003).

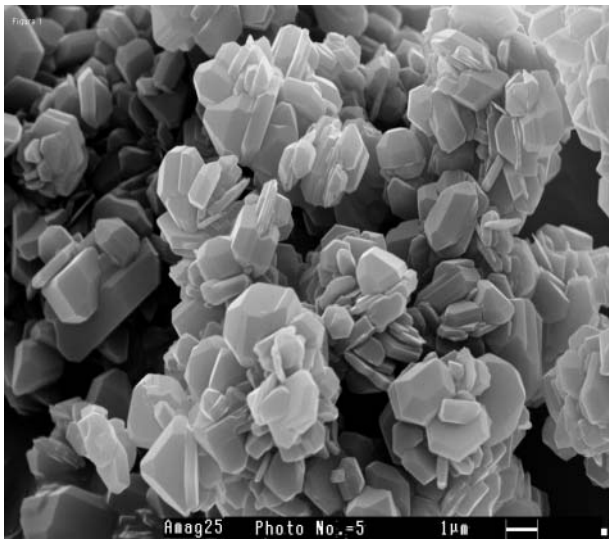

FIGURE 1. SEM image of the Amag25 gibbsite sample recorded in the secondary electron mode with a SEM LEICA Stereoscan 44 camera (beam current of 150 pA and voltage of 20 kV). Note the distribution of particle shapes from nearly equant particles to thick plates.

RESULTS AND DISCUSSION

Gibbsite crystallizes in space group $P2_1/n$. The experimental cell parameters are a = 8.684, b = 5.078, and c = 9.736 Å, β = 94.54°, and the unit cell contains eight $Al(OH)_3$ units (Saalfeld and Wedde 1974). The centrosymmetric structure of gibbsite can be described as a regular stacking of two-layer units, each dioctahedral layer being related to the neighboring one by a horizontal glide plane. In the structural optimization, the unit-cell geometry was homothetically relaxed. The relaxed cell parameters were a = 8.742, b = 5.112, and c = 9.801 Å, which corresponds to a 0.7% relative increase of the cell parameters. The residual pressure over the cell was 0.2 GPa. Atomic positions were relaxed with the $P2_1/n$ symmetry constraint (Table 1). The unit cell contains six non-equivalent OH groups. Their theoretical bond length ranges from 0.979 to 0.987 Å and from 0.991 to 0.994 Å, for in-plane (OH1, OH2, OH4) and out-of plane (OH3, OH5, OH6) OH groups, respectively. These bond lengths correspond to a systematic increase of c.a. 0.006 Å relative to those calculated by Gale et al. (2001) using the experimental geometry of heavy atoms reported by Saalfeld and Wedde (1974).

TABLE 1. Fractional relaxed atomic coordinates of gibbsite

Atom	x	y	z
Al1	0.168	0.531	–0.003
Al2	0.336	0.025	–0.003
O1	0.174	0.219	–0.112
O2	0.669	0.655	–0.103
O3	0.498	0.133	–0.106
O4	–0.020	0.632	–0.108
O5	0.303	0.716	–0.105
O6	0.822	0.146	–0.102
H1	0.072	0.138	–0.123
H2	0.574	0.551	–0.102
H3	0.494	0.108	–0.207
H4	–0.049	0.817	–0.113
H5	0.300	0.718	–0.206
H6	0.807	0.162	–0.203

TABLE 2. Infrared active OH stretching modes of gibbsite

Symmetry	Contribution*	TO frequency (cm^{-1})	LO frequency (cm^{-1})	Exp. (cm^{-1})
B_u	H5,H6	3317		
B_u	H5,H6	3334		
A_u	H3,H5,H6	3335	3347	3373
A_u	H5,H6	3351		3394
B_u	H3	3372		
A_u	H3,H6	3379	3458	3455
A_u	H4	3497		3514
B_u	H4	3497		
A_u	H2	3510		3526
B_u	H2	3511		
A_u	H1	3618		3621
B_u	H1	3620		

* Labels refer to Table 1.

The diagonalization of the analytical part of the dynamical matrix of gibbsite leads to 165 normal vibrational optical modes. The 24 modes involving the stretching of OH bonds are reported in Table 2 (IR active modes), 3 (Raman active modes), and 4 (Mode eigenvectors, electronic dielectric tensor, Born effective charge, and Raman tensors; MSA depository). The vibrations of non-equivalent in-plane OH groups are not coupled to each other. In contrast, a significant coupling was observed for the modes involving out-of-plane OH groups, except for the fully symmetric modes (A_g). As expected from geometrical considerations, the frequency of the modes related to the shorter in-plane OH groups is higher (> 3480 cm^{-1}) than that of the modes involving out-of-plane OH groups.

The theoretical infrared spectrum of gibbsite (Fig. 2) was derived considering two limiting cases for the particle geometry: platy particles perpendicular to **c*** and spherical particles. The theoretical spectra were computed using $\varepsilon_{ext} = 1$ as in Balan et al. (2005). They are compared with the resonances of the trace of the imaginary part of the dielectric tensor Im(ε(ω)). These resonances correspond to the transverse optical (TO) modes of an infinite crystal. Therefore, this comparison enables one to quantitatively determine the influence of the particle shape on the infrared spectrum.

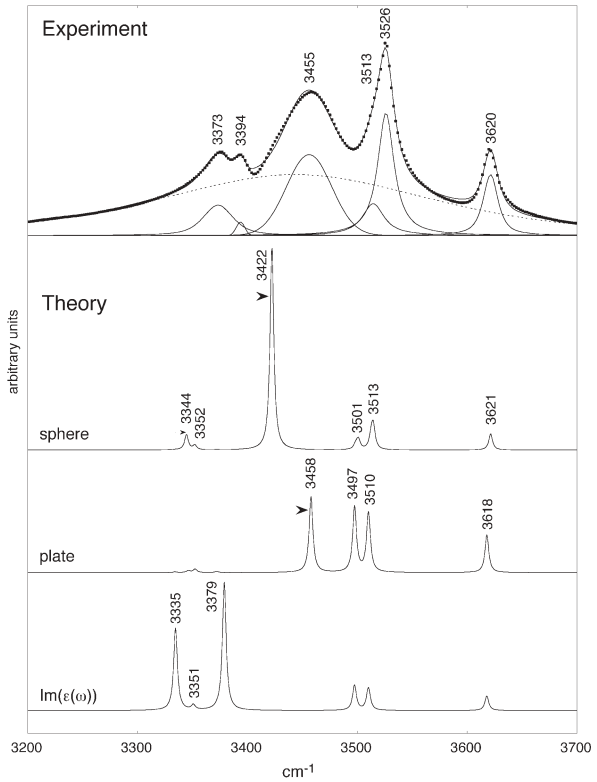

FIGURE 2. Experimental and theoretical infrared absorption spectrum of gibbsite in the range of the OH-stretching bands. The experimental spectrum has been decomposed in discrete absorption bands using a least-squares minimization procedure. The theoretical spectra have been computed for a spherical and for a thin platy particle shape. The imaginary part of the dielectric tensor computed for an infinite crystal (bottom) evidences the effect of the depolarization field occurring in small platy or spherical particles (horizontal arrows).

We first considered small platy particles with basal planes perpendicular to c*. As previously observed for kaolinite (Balan et al. 2001), this geometry has a maximum influence on modes with a strong polarization parallel to c*, whereas in-plane modes are mostly unaffected. The absorption bands due to out-of-plane modes were observed in the theoretical spectrum of the thin platy particle at the longitudinal optical (LO) mode frequency of the infinite crystal (Farmer 2000; Balan et al. 2005). In particular, the mode with a TO frequency of 3379 cm^{-1} corresponds to a band observed at 3458 cm^{-1} in the theoretical spectrum. This shift of 79 cm^{-1} is significantly higher than the maximum LO-TO splitting value of 30 cm^{-1} predicted by Gale et al. (2001) using an interatomic potential model. The strong resonance at 3335 cm^{-1} in Im(ε(ω)) is observed at 3347 cm^{-1}, corresponding to a LO-TO splitting of 12 cm^{-1}. In addition, the relative intensity of the shifted absorption bands significantly decreases compared with that of the unaffected bands.

The theoretical spectrum of small spherical particles differs significantly from that computed for the thin platy particles (Fig. 2). The shift of the bands related to modes with a polarization parallel to c* is smaller (9 and 43 cm^{-1} vs. 12 and 79 cm^{-1}, respectively) and their intensity is increased. The intensity and frequency of the other bands are affected.

We now compare the theoretical spectrum with its experimental counterpart (Fig. 2). The experimental infrared spectrum of gibbsite displays well-defined bands in the region of OH-stretching frequencies. Beside a broad baseline likely related to the defective structure of the sample and/or adsorbed water molecules, the least-squares fitting of the spectrum enables one to identify six bands, in excellent agreement with the previous observations of Wang and Johnston (2000). Note that according to these previous observations, a temperature decrease from 300 to 12 K only induces relatively small changes in the spectral shape. The most pronounced shift is observed for the OH-stretching mode at the lowest frequency, which is blue-shifted by 15 cm^{-1} (Wang and Johnston 2000).

The best agreement between theory and experiment was obtained for a spherical particle shape (Fig. 2). The three bands at 3620, 3526, and 3513 cm^{-1} were correctly predicted considering both their frequency and relative intensity. The broad and intense band at 3455 cm^{-1} corresponds to the peak calculated at 3422 cm^{-1}. As explained above, this peak is strongly influenced by the particle shapes. Therefore, the large width of the experimental peak most likely reflects the distribution of particle shape observed in the sample (Fig. 1) and supports the above assignment. The blue-shift of this band as a function of particle thinness has been experimentally observed on a series of synthetic gibbsite samples which exhibits a strong correlation between the relative intensity of the band component at 3460 cm^{-1} and the specific lateral surface area of the sample (Phambu et al. 2000). This correlation led Phambu et al. (2000) to incorrectly assign the band at 3460 cm^{-1} to the vibration of surface species present on the particle edges. Still considering the band widths, the narrow and broad experimental peaks at 3394 and 3373 cm^{-1}, respectively, correspond to those computed in the spectrum of the spherical particle at 3352 and 3344 cm^{-1}, respectively. Indeed, the peak at 3352 cm^{-1} is almost unaffected by the particle shape, whereas that

at 3344 cm^{-1} corresponds to a blue-shift of 9 cm^{-1} with respect to the TO frequency.

The proposed assignment is also consistent with the observation that the two bands at 3373 and 3455 cm^{-1} exhibit the most important inter-sample variations. For example, they were observed by Wang and Johnston (2000) at 3376 and 3463 cm^{-1}, respectively, whereas their other peaks have the same frequency as in the present study, within one wavenumber.

The Raman spectrum of a gibbsite single crystal was calculated by considering the electric field polarization and scattering geometry reported by Wang and Johnston (2000) (Fig. 3). A very good agreement between our theoretical results and the experimental observations of Wang and Johnston (2000) was obtained for the spectra probing the diagonal elements of the Raman tensors. The corresponding vibrational modes have A_g symmetry (Table 3). The frequency order of the three peaks observed at 3623, 3526, and 3519 cm^{-1}, together with the variation of their relative intensity as a function of the experimental geometry, is correctly reproduced by the peaks at 3614, 3506, and 3494 cm^{-1}, respectively. The peak experimentally observed at 3433 cm^{-1} corresponds to that calculated at 3388 cm^{-1}. According to their relative intensity, the peaks at 3370 and 3363 cm^{-1} most likely correspond to those calculated at 3318 and 3334 cm^{-1}, respectively. Despite the inversion of the relative frequency order of these peaks, this assignment is consistent with the accuracy range observed in previous DFT calculations of the vibrational spectrum of hydrous phyllosilicates, which is typically better than 1% for the frequency and 10% for the intensity (e.g., Balan et al. 2005). With respect to the spectra probing off-diagonal elements of the Raman tensors, corresponding to modes with the B_g symmetry, the agreement is not so good. In fact, their theoretical intensity is 10 to 1000 times lower than that of spectra probing diagonal elements. Therefore, we suspect that the corresponding experimental spectra are in fact affected by depolarization effects, leading to a dominant contribution of diagonal elements to the experimental spectrum.

TABLE 3. Raman active OH stretching modes of gibbsite

Symmetry	Contribution*	TO frequency (cm^{-1})	Exp.† (cm^{-1})
A_g	H5	3318	3370
B_g	H5,H6	3330	
A_g	H6	3334	3363
B_g	H3,H5,H6	3349	
A_g	H3	3388	3433
B_g	H3,H5,H6	3463	
A_g	H4	3494	3519
B_g	H4	3494	
B_g	H2	3506	
A_g	H2	3506	3526
B_g	H1	3614	
A_g	H1	3614	3623

* Labels refer to Table 1.
† Wang and Johnston (2000).

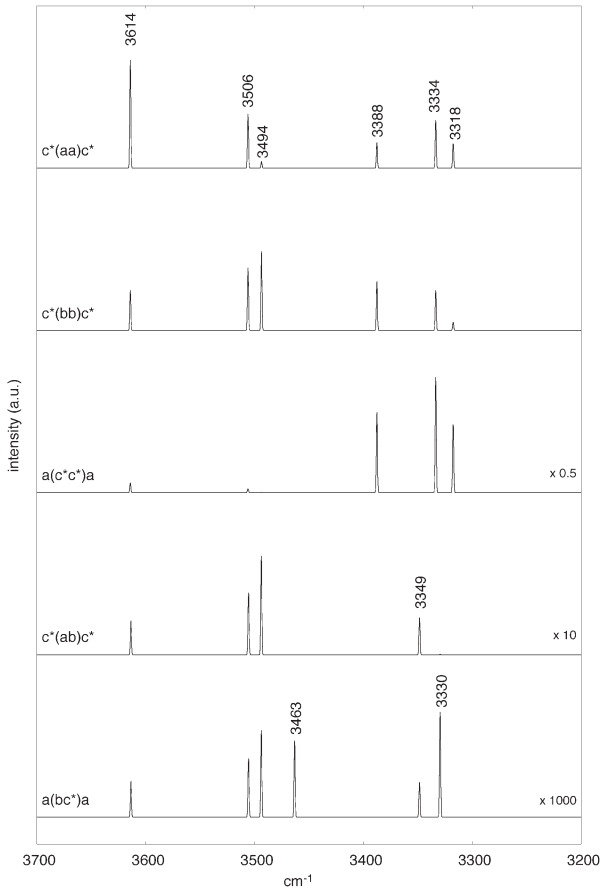

FIGURE 3. Theoretical Raman spectra of gibbsite calculated for the scattering geometries reported by Wang and Johnston (2000).

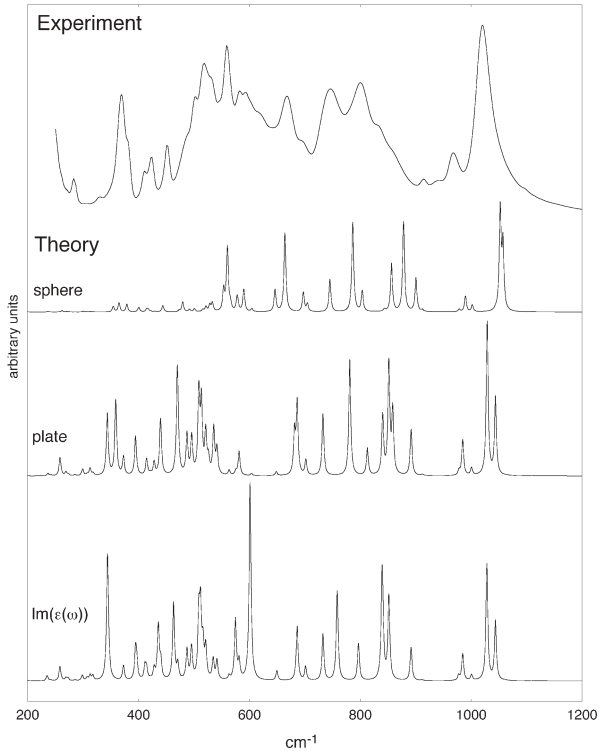

FIGURE 4. Experimental and theoretical infrared absorption spectrum of gibbsite in the mid IR range. The theoretical spectra have been computed for a spherical and for a thin platy particle shape. The imaginary part of the dielectric tensor computed for an infinite crystal (bottom) evidences the effect of the depolarization field occurring in small platy or spherical particles.

The existence of a linear dependence between the IR or Raman frequency of OH-stretching modes and the length of OH bonds in phases with octahedral Al has been previously suggested (Kubicki and Apitz 1998). Our calculations for gibbsite, as well as those for the kaolinite-group minerals (Balan et al. 2005), support this suggestion. In gibbsite, the frequency of modes involving shorter in-plane OH groups is indeed higher than that of modes involving longer out-of-plane OH groups. However, our results show that some band frequencies strongly depend on the macroscopic shape of the particles. A given OH group (e.g., OH6) may also contribute to modes with significantly different frequencies (Tables 2 and 3). Therefore, the straightforward use of this linear dependence to infer accurate structural parameters from IR or Raman frequencies might be misleading.

Finally, we have also computed the theoretical infrared spectrum of gibbsite in the mid-IR frequency range (200–1200 cm^{-1}) (Fig. 4). However, in this case, the strong band overlap observed in the experimental spectrum together with the complexity and the sensitivity of the theoretical spectrum to variations of the particle shape prevent us from performing an unambiguous assignment of the experimental bands, except for the bands at 968 and 1018 cm^{-1} which are related to bending modes of OH groups.

ACKNOWLEDGMENTS

We thank J.D. Kubicki for his constructive comments. The synthetic gibbsite sample was kindly provided by the Pechiney company. S. Locati (IRD, University of Paris VI) is acknowledged for the IR measurements. We thank S. Lebrun (IMPMC, University of Paris VI) and Stéphane Borensztajn (LPLE, University of Paris VI) for the SEM imaging. Calculations were performed at the IDRIS institute (Institut du Développement et des Ressources en Informatique Scientifique) of CNRS (Centre National de la Recherche Scientifique). This work is IPGP contribution no. 2059.

REFERENCES CITED

Balan, E., Saitta, A.M., Mauri, F., and Calas, G. (2001) First-principles modeling of the infrared spectrum of kaolinite. American Mineralogist, 86, 1321–1330.

Balan, E., Saitta, A.M., Mauri, F., Lemaire, C., and Guyot, F. (2002) First-principles calculation of the infrared spectrum of lizardite. American Mineralogist, 87, 1286–1290

Balan, E., Lazzeri, M., Saitta, A.M., Allard, T., Fuchs, Y., and Mauri, F. (2005) First-principles study of OH stretching modes in kaolinite, dickite and nacrite. American Mineralogist, 90, 50–60.

Baroni, S., de Gironcoli, S., Dal Corso, A., and Giannozzi, P. (2001) Phonons and related crystal properties from density-functional perturbation theory. Reviews of Modern Physics, 73, 515–561.

Digne, M., Sautet, P., Raybaud, P., Toulhoat, H., and Artacho, E. (2002) Structure and stability of aluminum hydroxides: a theoretical study. Journal of Physical Chemistry B, 106, 5155–5162.

Farmer, V.C. (1974) The infrared spectra of minerals. Mineralogical Society, London.

——— (2000) Transverse and longitudinal crystal modes associated with OH stretching vibrations in single crystals of kaolinite and dickite. Spectrochimica Acta A, 56, 927–930.

Fleming, S.D., Rohl, A.L., Parker, S.C., and Parkinson, G.M. (2001) Atomistic modeling of gibbsite: Cation incorporation. Journal of Physical Chemistry B, 105, 5099–5105.

Gale, J.D., Rohl, A.L., Milman, V., and Warren, M.C. (2001) An ab initio study of the structure and properties of aluminium hydroxide: Gibbsite and bayerite. Journal of Physical Chemistry B, 105, 10236–10242.

Jodin, M.-C., Gaboriaud, F., and Humbert, B. (2004) Repercussions of size heterogeneity on the measurement of specific surface areas of colloidal minerals: Combination of macroscopic and microscopic analyses. American Mineralogist, 89, 1456–1462.

Johnston, C.T., Wang, S.-L., Bish, D.L., Dera, P., Agnew, S.F., and Kenney III, J.W. (2002) Novel pressure-induced phase transformation in hydrous layered minerals. Geophysical Research Letters, 10.1029/2002GL015402.

Kleinman, L. and Bylander, D.M. (1982) Efficacious form for model pseudopotentials. Physical Review Letters, 48,1425–1428.

Kubicki, J.D. (2001) Interpretation of vibrational spectra using molecular orbital theory calculations. In R.T. Cygan and J.D. Kubicki, Eds., Molecular Modeling Theory: Applications in the Geosciences, 42, p. 459–483. Reviews in Mineralogy and Geochemistry, Mineralogical Society of America, Chantilly, Virginia.

Kubicki, J.D. and Apitz, S.E. (1998) Molecular cluster models of aluminum oxide and aluminum hydroxide surfaces. American Mineralogist, 83, 1054–1066.

Lazzeri, M. and Mauri, F. (2003) First principles calculation of vibrational Raman spectra in large systems: Signature of small rings in crystalline SiO_2. Physical Review Letters, 90, 036401.

Liu, H., Hu, J., Xu, J., Liu, Z., Shu, H., Mao, K., and Chen, J. (2004) Phase transition and compression behavior of gibbsite under pressure. Physics and Chemistry of Minerals, 31, 240–246.

Perdew, J.P., Burke, K., and Ernzerhof, M. (1996) Generalized gradient approximation made simple. Physical Review Letter, 77, 3865–3868.

Phambu, N., Humbert, B., and Burneau, A. (2000) Relation between the infrared spectra and the lateral specific surface areas of gibbsite samples. Langmuir, 16, 6200–6207.

Ruan, H.D., Frost, R.L., and Kloprogge, J.T. (2001) Comparison of Raman spectra in characterizing gibbsite, bayerite, diaspore and boehmite. Journal of Raman Spectroscopy, 32, 745–750.

Saalfeld, H. and Wedde, M. (1974) Refinement of the crystal structure of gibbsite, $Al(OH)_3$. Zeitschrift für Kristallographie, 139, 129–135.

Tardy, Y. (1993) Pétrologie des latérites et des sols tropicaux. Masson, Paris.

Troullier, N. and Martins, J.L. (1991) Efficient pseudopotentials for plane-wave calculations. Physical Review B, 43, 1993–2006.

Wang, S.-L. and Johnston, C.T. (2000) Assignment of the structural OH stretching bands of gibbsite. American Mineralogist, 85, 739–744.

MANUSCRIPT RECEIVED FEBRUARY 21, 2005
MANUSCRIPT ACCEPTED MAY 3, 2005
MANUSCRIPT HANDLED BY KEVIN ROSSO